doi:10.1016/j.jmb.2005.11.030 J. Mol. Biol. (2006) 355, 968–979

JMB

Available online at www.sciencedirect.com

SCIENCE DIRECT®

ELSEVIER

Protein Translocation through the Anthrax Toxin Transmembrane Pore is Driven by a Proton Gradient

Bryan A. Krantz[1], Alan Finkelstein[2] and R. John Collier[1]*

[1]*Department of Microbiology and Molecular Genetics Harvard Medical School 200 Longwood Ave, Boston MA 02115, USA*

[2]*Department of Physiology and Biophysics, Albert Einstein College of Medicine, 1300 Morris Park Ave, Bronx, NY 10461, USA*

**Corresponding author*

Protective antigen (PA) from anthrax toxin assembles into a homoheptamer on cell surfaces and forms complexes with the enzymatic components: lethal factor (LF) and edema factor (EF). Endocytic vesicles containing these complexes are acidified, causing the heptamer to transform into a transmembrane pore that chaperones the passage of unfolded LF and EF into the cytosol. We show in planar lipid bilayers that a physiologically relevant proton gradient (ΔpH, where the endosome is acidified relative to the cytosol) is a potent driving force for translocation of LF, EF and the LF amino-terminal domain (LF_N) through the PA_{63} pore. ΔpH-driven translocation occurs even under a negligible membrane potential. We found that acidic endosomal conditions known to destabilize LF_N correlate with an increased translocation rate. The hydrophobic heptad of lumen-facing Phe427 residues in PA (or ϕ clamp) drives translocation synergistically under a ΔpH. We propose that a Brownian ratchet mechanism proposed earlier for the ϕ clamp is cooperatively linked to a protonation-state, ΔpH-driven ratchet acting *trans* to the ϕ-clamp site. In a sense, the channel functions as a proton/protein symporter.

© 2005 Elsevier Ltd. All rights reserved.

Keywords: translocation; proton gradient; translocase; protein unfolding; planar bilayers

Introduction

Transport across membranes of ions, small polar molecules, and macromolecules, such as proteins, is often facilitated by specific, integral membrane proteins. Membranes are particularly impermeable to soluble proteins, because of their size and their globular, amphipathic nature. To remain folded and soluble, proteins bury hydrophobic surface while exposing a charged, polar surface to water, but this polar surface is incompatible with the apolar membrane interior. Many bacterial toxins (e.g. anthrax, diphtheria, botulinum, and tetanus toxins) take advantage of the low pH conditions in the endosome of mammalian cells to transform their enzymatic components into a partially unfolded, molten globule (MG) form that can circumvent the barrier imposed by the membrane more readily.[1–3] These toxins chaperone the delivery of their unfolded enzymatic cargos using separate translocase domains or proteins that form transmembrane pores in the endosomal membrane.[4–7] In general, the role of these pores during translocation is unclear; the driving force and underlying mechanisms for the concerted unfolding and translocation reactions remain only vaguely defined.

The toxin from *Bacillus anthracis* is an ideal model system for the study of protein translocation across membranes, as it is composed of three separate proteins, a translocase and two substrates, that may be produced recombinantly in soluble form and studied independently.[8] Protective antigen (PA; 83 kDa), the translocase component, transports the two enzymatic components, lethal factor (LF; 90 kDa) and edema factor (EF; 89 kDa) to the cytosol. LF is a protease that cleaves mitogen-activated protein kinase kinases; EF is a Ca^{2+} and calmodulin-dependent adenylate cyclase. Toxin action is initiated by a self-assembly process. First, PA binds to a cell-surface receptor, where it is activated by a furin-family protease, and a small fragment dissociates. The remaining 63 kDa, receptor-bound portion (PA_{63}) self-assembles into a ring-shaped homoheptamer, called prepore. Prepore may then form complexes with up to

Abbreviations used: MG, molten globule; PA, protective antigen; LF, lethal factor; LF_N, LF amino-terminal domain; EF, edema factor; EF_N, EF amino-terminal domain.

E-mail address of the corresponding author: jcollier@hms.harvard.edu

0022-2836/$ - see front matter © 2005 Elsevier Ltd. All rights reserved.

three molecules of EF and/or LF. These complexes are endocytosed and delivered to an acidic compartment, where prepore undergoes an acidic pH-dependent conformational rearrangement to form a cation-selective, ion-conducting channel.[9] The PA_{63} channel, or pore, spans the membrane as an extended, 14-stranded β barrel,[10,11] and serves as the conduit for LF and EF into the cytosol.

A model of the PA_{63} 14-strand β barrel reveals that its lumen is ~15 Å wide and is able to accommodate secondary structure only as large as an α helix.[3] Translocation through the lumen thus requires the substrates to unfold.[3,12] Thermodynamic analysis of the conformational stabilities of the LF and EF homologous ~250 residue amino-terminal domains (LF_N and EF_N) indicates that acidic conditions encountered in the endosome are sufficient to destabilize the native structures of these proteins.[3] Also, a positive membrane potential ($+\Delta\psi$) can drive the acid-destabilized LF_N through the PA_{63} pore, where the amino terminus precedes the carboxy terminus into the pore.[4,13] However, *in vitro* and *in vivo* studies have shown that translocation is more complicated than acid-induced unfolding, as followed by electrophoresis through a passive pore. The translocase channel contains a required, solvent-exposed, lumen-facing heptad of Phe427 residues, or ϕ clamp, that can facilitate unfolding of the MG by interacting directly with the substrate and actively chaperoning hydrophobic sequences.[5] The ϕ clamp grasps hydrophobic sequences as they unfurl from the MG substrate to direct the translocating chain through the channel. But how does PA_{63}, a cation-selective channel, accommodate the LF_N anionic side-chains, which outnumber its cationic counterparts? Clearly, the glutamate and aspartate residues must be at least sufficiently protonated in the channel to impart a net positive charge on LF_N, otherwise we would have the thermodynamically impossible situation of a negatively charged LF_N being driven across the membrane by $a+\Delta\psi$ without a compensatory dissipative process. Beyond this, how does the acid-induced destabilization of the substrate couple with translocation? Can the proton gradient (ΔpH) established across the endosomal membrane provide enough driving force to support protein translocation? Here, we address these issues.

Results and Discussion

Symmetric pH

pH-dependence of translocation

Previous planar lipid bilayer studies demonstrated that LF_N could be translocated through PA_{63} channels under a $\Delta\psi$ of +50 mV at symmetric pH 5.5, but not pH 6.6.[4] (The membrane potential is defined as $\Delta\psi=\psi_{cis}-\psi_{trans}$, where $\psi_{trans}\equiv 0$ mV.) This observation is consistent with the acidic pH-induced conformational destabilization described for LF_N and EF_N,[3] implying that partial unfolding to an MG form is kinetically linked to more rapid translocation. Extending these studies, we examined the rates of translocation at different symmetric pH values. In planar bilayer experiments, LF_N was added to the *cis* compartment, where it bound to PA_{63} channels and blocked ion conductance through the channel. Following perfusion of the *cis* compartment to remove unbound LF_N, the $\Delta\psi$ was stepped to a higher positive voltage, and the rate of translocation was monitored by the increase in channel conductance as LF_N passed through the channel (Figure 1(a)). We observed that when the *cis* and *trans* pH values were raised symmetrically from acidic pH to more neutral pH, the rate of LF_N translocation decreased correspondingly (Figure 1(b) and Table 1). For example, at +50 mV the translocation half-time was ~5 s at symmetric pH 5.5 and 36 s at symmetric pH 6.0; at symmetric pH 6.6, translocation was too slow to measure, even at +70 mV.

pH-dependence of LF_N stability and rate of translocation correlate

We recorded the kinetics of LF_N translocation through PA_{63} channels at a $\Delta\psi$ of +60 mV and pH values from ~5 to 6.5 (Figure 1(b)) and measured the translocation half time, $t_{½}$, as a simple indicator of the complex series of rate constants describing the entire S-shaped translocation kinetics. For each pH value tested, an approximate translocation activation energy ($\Delta G^{\ddagger}_{transl}$) was calculated from the half-times as $\Delta G^{\ddagger}_{transl} = RT \ln t_{1/2}^{-1}$. This quantity was plotted against the pH-dependence of the free energy difference (ΔG_{NI}) observed for LF_N between its native (N) and MG intermediate (I) conformations, using:

$$\Delta G_{NI}(\mathrm{pH}) = RT\ln(K_{NI}^{\mathrm{pH8}}[(1+10^{\mathrm{p}K_N-\mathrm{pH}})/(1+10^{\mathrm{p}K_I-\mathrm{pH}})]^n)$$

the known equilibrium stability between the N and I states, K_{NI}^{pH8} (at a reference pH of 8), and the previously defined proton dissociation constants, p*K*, for the *n* titratable groups responsible for destabilizing LF_N upon protonation.[3] The pH-dependent changes in ΔG_{NI} and $\Delta G^{\ddagger}_{transl}$ were well correlated, with a slope of unity (1.0 (±0.1)) (Figure 1(c)). Thus, translocation kinetics correlated strongly with the global stability of the translocating substrate, LF_N.

Because the correlation of the translocation activation energy (deduced from the translocation $t_{½}$) and the pH-dependence of the conformational stability covers two orders of magnitude (Figure 1(c)), we infer that the pH-induced destabilization of the native state and subsequent population of an MG state limits translocation. For it is unlikely that the p*K* and the number of titratable groups responsible for conversion of LF_N to the MG state exactly match other distinct titratable groups in PA_{63} or LF_N that solely affect

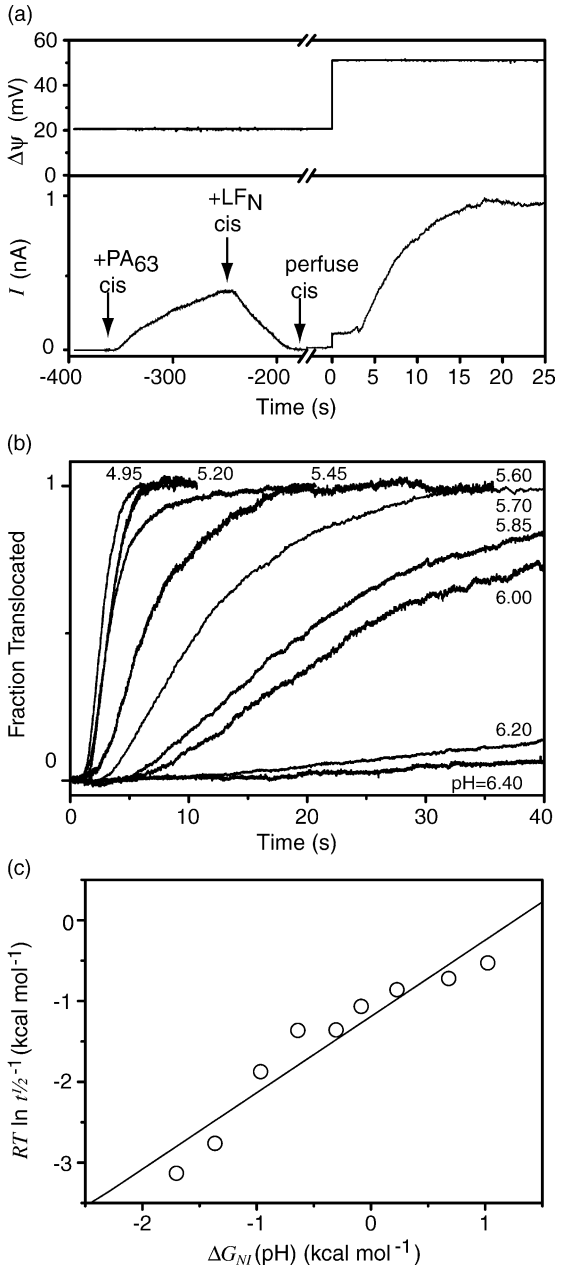

Figure 1. Symmetric pH-dependence of LF_N translocation kinetics through PA_{63} channels. (a) In a typical Δψ-step protein translocation experiment, the *cis* and *trans* compartments contained 100 mM KCl, 1 mM EDTA, and either 5 mM potassium succinate or universal bilayer buffer (UBB: 10 mM phosphate, 10 mM Mes, and 10 mM oxalic acid) at pH 5.5 at room temperature. Prepore heptameric PA_{63} (final concentration ~2 pM) was first added to the *cis* compartment at $\Delta\psi = +20$ mV (where $\psi_{trans} \equiv 0$) until channel formation reached steady state (indicated by the stabilization of the current). LF_N (final concentration ~3 nM) was then added to the *cis* compartment until the current was blocked; the *cis* compartment was then perfused of unbound LF_N. At time zero, Δψ was stepped to the final voltage of +50 mV ($\Delta\psi_{final}$), and LF_N translocation kinetics through the PA_{63} channel were indicated by the increase in conductance *versus* time. (b) Kinetic transients as in (a) for LF_N translocation ($\Delta\psi_{final} = +60$ mV) when the *cis* and *trans* compartments were bathed symmetrically in UBB at the indicated pH values. (c) Correlation of the symmetric pH-dependence of LF_N translocation kinetics from (b) at a $\Delta\psi = +60$ mV (given as an activation free energy of $RT \ln t_{1/2}^{-1}$) to the pH-dependence of the conformational stability of LF_N, or ΔG_{NI}(pH), using previously determined stability values.[3] The relation is fitted to a straight line, which has a slope of 1.0(±0.1), and a correlation *R*-value of 0.95.

Table 1. Half-times of LF_N translocation at symmetric pH

$\Delta\psi_{final}$ (mV)	$t_{½}$ (s)				
	pH 5.2	pH 5.5	pH 5.7	pH 6.0	pH 6.2
25	75				
30	22				
35	16				
40	7	13	35		
45	6	8	20		
50	5	5	10	36	
60		3	4	15	28
70		1.5	3	9	18
75					12

Under the indicated symmetric pH conditions, Δψ was stepped from +20 mV to the indicated $\Delta\psi_{final}$ to initiate LF_N translocation. The translocation half-times ($t_{½}$) were obtained from records such as those in Figure 1(b).

translocation. Moreover, when fold-stabilizing co-solvents were added to the *cis* compartment of the bilayer, the translocation rate slowed (Supplementary Data, Figure S1).

pH gradient

Proton gradients drive LF_N translocation through PA_{63} channels

We found that translocation of LF_N (Figure 2(a)), as well as full-length LF (Figure 3) and EF (Supplementary Data, Figure S2), through PA_{63} channels was markedly stimulated by a proton gradient (ΔpH); that is, when the pH of the *trans* side (pH_{trans}) of the lipid bilayer was greater than that of the *cis* side (pH_{cis}). The proton gradient is defined as:

$$\Delta pH = pH_{trans} - pH_{cis}$$

The following experiments illustrate this:

(1) At a low Δψ of +20 mV, no translocation occurred at pH 5.5, if the ΔpH = 0, whereas there was rapid translocation when the *trans* pH was raised to 6.2 (Figure 2(a)).
(2) Translocation was inhibited (or slowed) when pH_{cis} was greater than pH_{trans} (i.e. ΔpH was negative; Figure 4).
(3) Other ΔpH values, at pH_{cis} higher than 5.5, and even above neutrality, were effective in promoting translocation, so long as pH_{trans} was greater than pH_{cis}. Thus, raising pH_{trans} from 8.5 to 8.8 still increased the translocation rate about twofold (Figure 5).

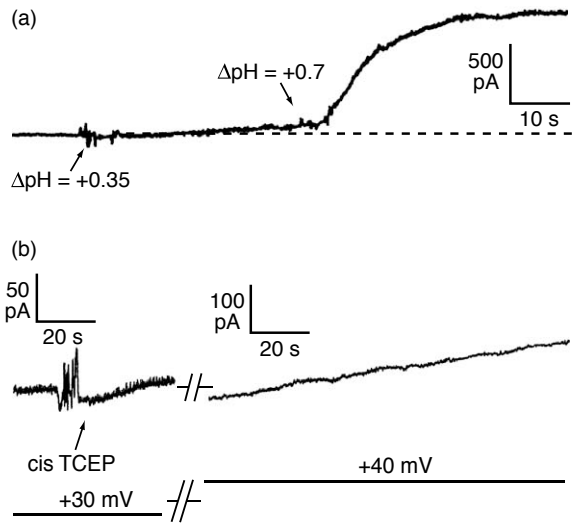

Figure 2. The effect of raising pH_{trans} on LF_N translocation. (a) In an example of an LF_N translocation experiment driven by a ΔpH jump, the *cis* and *trans* compartments were initially bathed in symmetric pH 5.5 (5 mM potassium succinate, 100 mM KCl, 1 mM EDTA) at a Δψ of +20 mV. PA_{63} channel conductance was 97% blocked by the addition of LF_N (final concentration 3.3 nM) (as in Figure 1(a)). The record begins after perfusion of the *cis* compartment under a constant Δψ of +20 mV. At the first arrow, pH_{trans} was raised to 5.85 (with 3.3 mM potassium phosphate); a slow rate of rise in conductance was seen, reflecting the translocation of LF_N. At the second arrow, pH_{trans} was raised to 6.2 (with 6.6 mM potassium phosphate), causing a much greater increase in the rate of LF_N translocation. The $t_{½}$ of ~6 s at pH 6.2 likely underestimates the rate of LF_N translocation, as the kinetics are limited by the buffer mixing dead-time. (b) In symmetric pH 6.7 buffer (10 mM potassium dimethylglutarate (DMG), 100 mM KCl, 1 mM EDTA), PA_{63} channels were formed (as in Figure 1(a)). After a steady-state conductance was reached, LF_N-biotin (LF_N with biotin attached near its C terminus[4]) was added to the *cis* compartment (~3 nM), blocking channel conductance 98%. Streptavidin was then added to the *cis* compartment (10 μg/ml). pH_{trans} was raised from 6.7 to 8.0 (with 5 mM Ches), and the *cis* compartment was perfused. After stepping the Δψ to +40 mV, there was a very slow rise in conductance (~1.5-fold in 80 s). The Δψ was then stepped back to +30 mV. The record begins here with no discernible rise in the conductance, despite a Δψ of +30 mV and a ΔpH of 1.3. However, once Tris(2-carboxyethyl)-phosphine (TCEP) (which reduces the disulfide bond linking biotin to LF_N and thereby frees LF_N of liganded streptavidin) was added to the *cis* compartment (2.5 mM), there was a continuous rise in conductance, reflecting LF_N translocation through the channel. (The break in the record is 27 s; note the change in current scale after the break.)

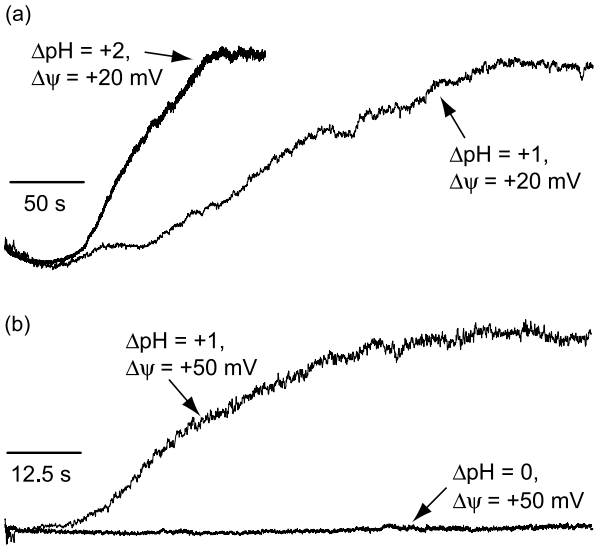

Figure 3. Whole LF translocation is driven by a ΔpH. For whole LF translocation experiments, PA_{63} channels were formed as in Figures 1(a) and 2(a), and 25 nM LF was added to the *cis* compartment to block conductance to > 95%. (a) LF translocation was recorded at a Δψ of +20 mV and either a one-unit or two-unit ΔpH, where pH_{cis} was 5.5 in both cases. (b) LF translocation was recorded both under a Δψ alone (+50 mV) and under the same Δψ plus a one-unit ΔpH (pH_{cis}=5.5, pH_{trans}=6.5). Note that there was virtually no translocation of whole LF with a Δψ = +50 mV, in the absence of a pH gradient. The current scales are normalized to overlay the records.

It is possible, but unlikely, that the rise in conductance induced by raising pH_{trans} (e.g. Figure 2(a)) resulted from LF_N dissociating into the *cis* compartment, rather than translocating to the *trans* compartment. As a control, we added LF_N-biotin (LF_N with biotin attached near its C terminus) and streptavidin to the *cis* compartment. When streptavidin binds LF_N-biotin, the streptavidin moiety does not prevent LF_N from entering and blocking the PA_{63} channel,[13] but it does prevent translocation.[4] As expected, raising pH_{trans} under these conditions did not cause the conductance to rise, but subsequent addition of a reducing agent to the *cis* solution, which broke the disulfide bond linking biotin (with its attached streptavidin) to LF_N, led to the expected rise in conductance, reflecting LF_N translocation under the ΔpH condition (Figure 2(b)).

Translocation of whole LF and EF is driven by ΔpH

Under acidic conditions known to be destabilizing for LF_N and EF_N (symmetric pH 5.5) and a moderate +Δψ of 50 mV, little translocation of whole LF or EF occurred; however, introduction of a ΔpH resulted in significant translocation (Figure 3(b) and Supplementary Data, Figure S2). Even at a low Δψ of 20 mV, ΔpH promoted translocation of LF in a ΔpH-dependent manner; i.e. larger +ΔpH caused more rapid translocation (Figure 3(a)). The conditions of low Δψ and a ΔpH, as in Figure 3(a), are particularly relevant to the conditions existing for LF (and EF) bound to a PA_{63} pore in an acidic endosome, and hence these experiments have particular biological relevance.

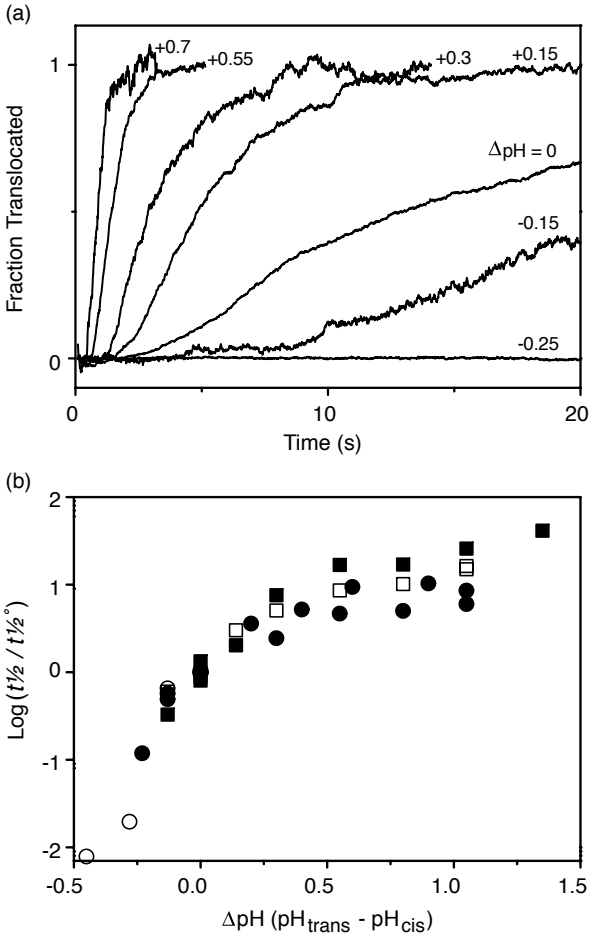

Figure 4. Translocation is controlled by the magnitude and sign of the ΔpH. (a) LF_N translocation driven at the indicated ΔpH values (where $\Delta pH = pH_{trans} - pH_{cis}$). pH_{cis} was held at a constant value of 5.45 for each transient. The *cis* and *trans* compartments were initially bathed in UBB (pH 5.45), and the indicated ΔpH was established by either raising or lowering pH_{trans} with 2 M KOH or 1 M HCl. PA_{63} channels were formed at a Δψ of +20 mV and blocked by LF_N (20 nM) at a Δψ of +1 mV. The *cis* compartment was then perfused, and at time zero, Δψ was stepped to +45 mV to initiate translocation. (b) Using the $t_{½}$ values of these and other translocation transients (where pH_{cis} was held at a constant value of 5.45), the logarithm of the ratio of the $t_{½}$ in the presence and in the absence of a ΔpH ($t_{½}$ and $t_{½}°$, respectively), are plotted against the final ΔpH condition. The ratio comparisons were made at four different constant Δψ values indicated by symbols as +40 (■), +45 (□), +50 (●), and +60 mV (○).

Δψ-driven versus *ΔpH-driven translocation*

In comparing the Δψ dependence of LF_N translocation in the presence and in the absence of a one-unit ΔpH ($pH_{trans} = 6.5$, $pH_{cis} = 5.5$), the ΔpH was better able to promote translocation at lower voltages than at higher voltages (Figure 6(a)). Moreover, extrapolating the translocation $t_{½}$ back to 0 mV, we found that this ΔpH would accelerate translocation ~100-fold relative to the rate expected in the absence of Δψ. The ΔpH condition ($pH_{trans} = 6.5$, $pH_{cis} = 5.5$) is offset 60 mV or more from the symmetric pH 5.5 condition (Figure 6(a)). The offset is of the order of the value expected for a chemical gradient.

Fold-stabilizing gradients do not drive LF_N translocation

At first glance, it would appear that the re-folding of LF_N that is promoted by the higher *trans* pH, as LF_N emerges into that solution, could be acting as a driving force on translocation, trapping the re-folded protein on the *trans* side and thereby, in addition to the transmembrane voltage, adding another vectorial component to the process. This appears to be an unlikely explanation of the *trans* pH effect, however, because a refolding reagent such as 1 M glucose did not stimulate translocation when added to the *trans* side (Supplementary Data, Figure S1).

Glucose and other "protecting osmolytes" have been shown to stabilize proteins, and cause even "random coil" proteins to collapse into more compact structures.[14] Equilibrium denaturant titrations of a fluorescently labeled form of LF_N (LF_N^*) that is capable of fluorescence resonance energy transfer when folded confirmed that 1 M glucose stabilized LF_N (Supplementary Data, Figure S1). At pH 7.5, the N state was stabilized ~1 kcal mol^{-1} relative to the I state (or MG conformation); the I state was stabilized ~0.7 kcal mol^{-1} over the more expanded, partially unfolded form (referred to as the J state). Although the addition of 1 M glucose to the *cis* compartment slowed translocation (about threefold) as expected, the addition of 1 M glucose to the *trans* compartment failed to stimulate translocation and instead slowed it about twofold (Supplementary Data, Figure S1). For the secondary and tertiary structure-stabilizing co-solvent, 2,2,2-trifluoroethanol,[15] we found that *cis*-side addition at 5% (w/v) slowed the rate of translocation about threefold (at symmetric pH 5.5, +50 mV), whereas *trans*-side addition had no effect on the translocation rate (Supplementary Data, Figure S1).

The slowing of LF_N translocation by non-electrolytes in the *cis* compartment that stabilize its native structure is consistent with the correlation of the rate of LF_N translocation with the pH-dependence of its conformational stability (Figure 1(c)). However, since the addition to the *trans* side of non-electrolytes that increase the stability of LF_N at either the secondary or tertiary structural level did not stimulate translocation, the stimulatory effect of raising the *trans* pH cannot be attributed to its promoting the re-folding of LF_N.

"Unfolding" and "translocation" barriers

Although we expect that a protein must unfold and shed its residual tertiary structure in order to

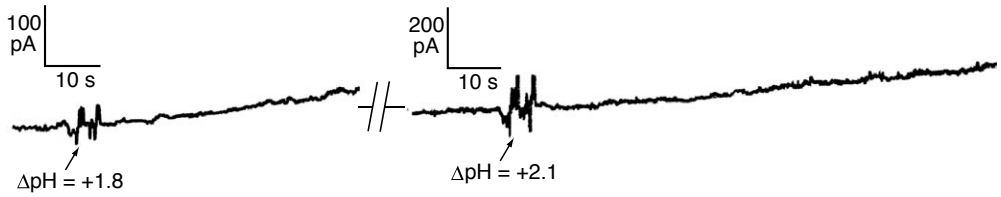

Figure 5. LF_N translocation is stimulated at $pH_{trans} > 8$. In symmetric pH 6.7 solutions (10 mM DMG), PA_{63} channels were formed and conductance blocked (98%) by LF_N (6.6 nM) as in Figure 1(a). The *cis* compartment was then perfused of unbound LF_N at a $\Delta\psi$ of +20 mV. Following perfusion, pH_{trans} was raised to 8.2 with 10 mM Ches buffer, and the $\Delta\psi$ was stepped to +25 mV. The plotted record begins at this point with a ΔpH of +1.5 and a slow rate of rise of conductance. Increasing pH_{trans} to 8.5 (first arrow, ΔpH of +1.8) with 11.7 mM Ches, initiated an increase in the rate of conductance rise (i.e. LF_N translocation rate). Moreover, raising pH_{trans} to 8.8 (second arrow, ΔpH of +2.1) with 14.2 mM Ches caused an additional increase in the translocation rate. (The break in the record is 70 s; note the change in current scale after the break.)

pass through the narrow channel, we do not know the timescales of the pH-induced unfolding and refolding reactions on the surface of PA_{63}. We have characterized only the translocation kinetics using the $t_{½}$ and not the more elemental kinetic rate constants. To simplify our discussion, however, we will define energy barriers, acknowledging that the observed translocation kinetics are S-shaped, multi-exponential, and complex. The barrier diagrams presented in Figure 8 are intended to represent the energy surface that unfolded polypeptide encounters as it unravels from the MG state and subsequently travels through the channel. We expect, of course, that multiple kinetic steps are implied by the periodicity of hydrophobicity, hydrophilicity, and charge over the length of the LF_N sequence (Figure 9(a)).

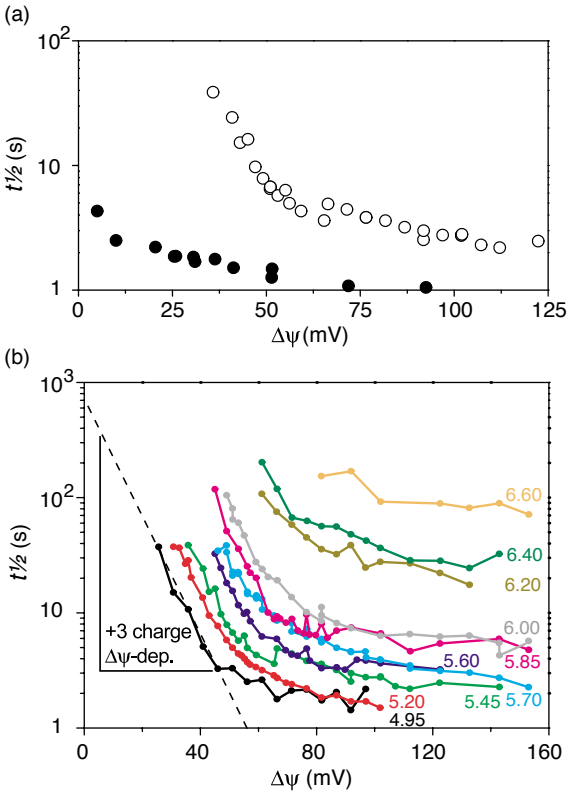

Figure 6. The $\Delta\psi$ dependence of LF_N translocation kinetics. (a) $\Delta\psi$ dependence of LF_N translocation kinetics in the presence (●) and in the absence (○) of a ΔpH = +1 (pH_{cis} 5.5). (b) $\Delta\psi$ dependence of the rate of LF_N translocation (indicated by the $t_{½}$) at the indicated symmetric pH conditions. The indicated slope of the $\Delta\psi$ dependence of the logarithm of $t_{½}$ is equivalent energetically to the presence of about +3 charges in the rate-limiting species within the PA_{63} channel. Note the plateauing of $t_{½}$ at large $\Delta\psi$.

Figure 8 depicts a two-barrier, one-well scheme proposed previously,[5] in which translocation may be limited by the equilibrium population of a required, partially unfolded species (akin to the MG state observed in solution). Unfolding exposes sequence dense in hydrophobic and cationic sites that threads into and forms the observed intermediate complex with the ϕ clamp.[5] The ϕ clamp defines an energy well that partitions the "unfolding reaction" in the *cis*-side "cap" of the PA_{63} channel from a *trans*-side "translocation barrier" in the extended β barrel. At low $+\Delta\psi$ or $\Delta pH \leq 0$, the translocation barrier is the major barrier. But in this sequential reaction, translocation requires unfolded protein sequence to be in the ϕ clamp and thereby is modulated thermodynamically by the stability of the protein substrate. At higher voltage and larger ΔpH, translocation is kinetically limited (Figures 4(b) and 6). Thus, the translocation barrier is lowered such that a separate barrier kinetically controls translocation: this barrier is both largely $\Delta\psi$ and ΔpH-independent, and is likely related to the protein unfolding reaction in the *cis*-side cap. In summary, two separate steps (or barriers) are needed to describe the observed $\Delta\psi$ and ΔpH dependence of the kinetics. We have termed them: a *cis*-side unfolding barrier that is affected by denaturing, acidic pH conditions or stabilizing co-solvents; and a *trans*-side translocation barrier, modulated by either $\Delta\psi$ or ΔpH.

PA_{63} ϕ-clamp mutants were less stimulated by a pH gradient

In an effort to identify residues lining the heptameric PA_{63} channel for their impact on

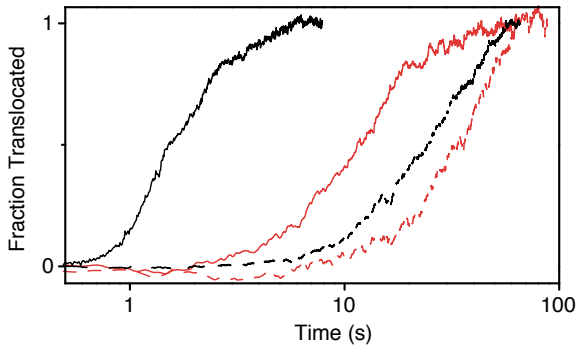

Figure 7. A PA_{63} ϕ-clamp mutation is defective in ΔpH-driven LF_N translocation. Kinetic records acquired as in Figures 1(a) and 4(a) for LF_N translocation through WT PA_{63} channels driven by Δψ alone (Δψ = +40 mV, ΔpH = 0 (symmetric pH 5.5); broken black line) or by Δψ and ΔpH (Δψ = +40 mV, ΔpH = +1 (pH_{cis} = 5.5); continuous black line) compared to translocation through F427A PA_{63} channels driven by Δψ alone (Δψ = +50 mV, ΔpH = 0 (symmetric pH 5.5); red broken line) or by Δψ and ΔpH (Δψ = +50 mV, ΔpH = +1 (pH_{cis} = 5.5); red continuous line). See Table 2 for additional data on ϕ clamp mutants under a ΔpH.

Table 2. The ΔpH rate-enhancement for a panel of ϕ clamp PA_{63} mutants

PA_{63} F427X	Δψ (mV)	$t_{½}$(Δψ) (s)	$t_{½}$(Δψ, ΔpH) (s)	ΔpH rate-enhancement (fold)
WT	+40	25	1.5	17
L	+40	74	2.8	26
W	+40	51	4.7	11
Y	+50	88	5	18
I	+50	41	8	5
A	+50	32	12	3
S	+50	83	18	5
D	+50	120	150	0.8

Translocation $t_{½}$ values were measured for LF_N driven through the PA_{63} F427X mutant channel by either a Δψ alone (at symmetric pH 5.5) or by both a constant Δψ (+40 to +50 mV) and a positive, one-unit ΔpH (pH_{cis} = 5.5, pH_{trans} = 6.5). The ΔpH rate-enhancement is defined by the ratio: $t_{½}$ (Δψ)/$t_{½}$ (Δψ, ΔpH). Each tested PA_{63} mutant was given equal opportunity to be stimulated by a ΔpH; i.e. not be limited by the known ΔpH-independent process (Figure 4(b)), so that the translocation rate under a Δψ alone had more or less consistent $t_{½}$ values (of the order of ~30 to 100 s). Despite this consideration, it is known[5] that at lower Δψ (less than +30 mV) the ΔpH rate-enhancement for WT and F427→(W, Y or L) PA_{63} channels would be even greater than that shown here (at +40 to 50 mV); but the mutants F427→(I, A, S, and D) are so defective that the quantitative comparison at these lower Δψ cannot be reported.

translocation, we showed earlier that the ϕ clamp, a site composed of a heptad of Phe427 residues, is required for translocation in cells and catalyzes translocation in planar lipid bilayers.[5] Here, we report that a ΔpH (pH_{cis} = 5.5, pH_{trans} = 6.5) was less able to accelerate translocation through F427A PA_{63} channels than through wild-type (WT) channels (Figure 7). By contrast, when F427Y PA_{63} (a functional ϕ-clamp variant) was tested, the ΔpH stimulated the rate of translocation ~20-fold (Table 2). A ΔpH was more effective in stimulating translocation when large aromatic and aliphatic residues (Phe, Trp, Leu) were present at position 427 than when smaller aliphatic or hydrophilic substitutions (Ile, Ala, Ser, Asp) were present at this position (Table 2)†.

How the ϕ clamp can maintain a ΔpH

Why is a + ΔpH less effective in driving translocation through PA_{63} channels with a mutated ϕ clamp (F427A) than through PA_{63} channels with a WT ϕ clamp, given that phenylalanine side-chains cannot be titrated? F427A PA_{63} channels are defective in stably binding the LF_N amino terminus, which flickers in and out of the channel, thereby allowing cations to pass through the channel,[5] and we presume that protons can likewise leak past the mutated F427A site. Thus, the WT ϕ clamp functions as a binding site for hydrophobic protein sequence, and may effectively maintain the proton gradient by acting as a hydrophobic seal. The higher concentration of proton in the *cis*-side cap, which is required to acid-destabilize LF_N, is kept separate from the lower concentration of proton *trans* to the ϕ clamp, which facilitates translocation (Figure 8).

What is titrated during ΔpH-driven translocation

Assuming that the ϕ clamp maintains the proton gradient, we expect that the residues titrated by the higher pH_{trans} are *trans* relative to the ϕ-clamp site. The residues that line the extended β barrel of the PA_{63} channel satisfy this criterion,[10] and we had begun testing their involvement in ΔpH-driven translocation. (Considering only charged residues and the 7-fold symmetry of the channel, 42 Asp or Glu and 14 His residues line the β barrel.) When pairs of His or Glu residues near the *trans*-most opening of the β barrel were doubly substituted with Thr, these mutant PA_{63} channels failed to disrupt ΔpH-driven translocation (unpublished results). Although we have not mutated all of the charged, lumen-facing residues lining the β barrel of the PA_{63} channel, we tentatively conclude that the titrated residues most affecting ΔpH-driven translocation reside not in the channel, but rather in the translocating substrate, LF_N‡.

† F427I PA is an exception to this generalization, as previously discussed.[5]

‡ We do not mean to imply that further mutagenesis in the β barrel would not eventually affect ΔpH-driven translocation. For example, loss of cation selectivity in the channel would be expected to impair ΔpH-driven translocation by the following model.

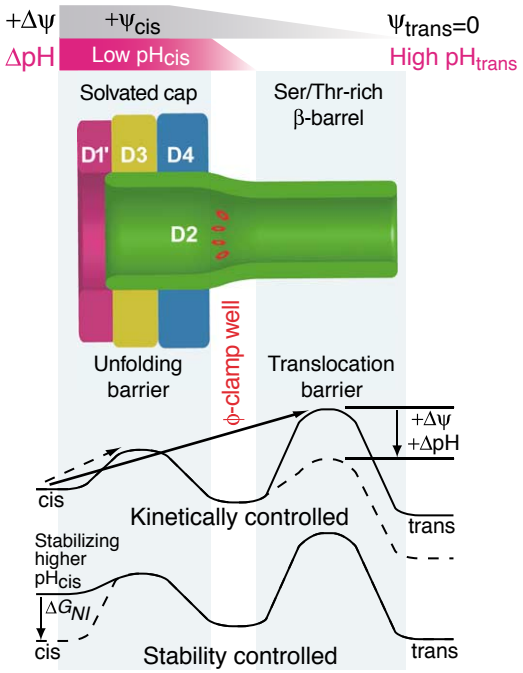

Figure 8. Structural and energetic models of translocation. Translocation energy diagrams with two barriers and one well modeled on a cross-sectional depiction of the PA_{63} channel colored by domain: D1′ (magenta), D2 (green), D3 (gold), and D4 (blue). The Phe427 ϕ clamp (red) defines an energy well for hydrophobic and cationic stretches of translocating polypeptide.[5] The Δψ gradient is indicated (at the top in gray) such that one-third of the voltage-drop occurs *cis* to the ϕ clamp.[5,30] The ΔpH is indicated (at the top in magenta) such that the ϕ clamp defines a boundary, since this hydrophobic site creates a seal blocking the passage of small ions,[5] partitioning higher pH conditions of the cytosolic (*trans*) side from lower acidic pH conditions on the endosomal (*cis*) side. In the energy diagrams (at bottom), the barrier on either the *cis* or *trans* side of the ϕ-clamp well, termed "unfolding barrier" and "translocation barrier," respectively, are shaded to indicate their location in the channel. Acidic pH conditions on the *cis* side of the ϕ clamp destabilize the substrate protein, allowing unfolded polypeptide chain to pass into the ϕ clamp. Either a favorable ΔpH or +Δψ can reduce the *trans*-side β-barrel translocation barrier. Translocation can be limited kinetically by the translocation barrier (continuous line arrow), but when this barrier is reduced by large Δψ or ΔpH, the unfolding barrier is rate-limiting (dotted line arrow), which is largely independent of Δψ and ΔpH. Alternatively, translocation may be dominated by the equilibrium stability of the substrate protein (affected by pH_{cis} conditions, as in Figures 1(c) and S1).

A charge-state ratchet translocation model

Here, we propose a novel charge-state Brownian ratchet mechanism for ΔpH-driven translocation based on the chemical asymmetry created by a ΔpH. Considering two degrees of conformational freedom in the backbone, a polypeptide chain such as LF_N would have ~150 kcal mol^{-1} of Brownian thermal energy available. This large pool of diffusive thermal energy, by its nature, cannot do useful work, such as driving the translocating chain through a transmembrane pore in a unidirectional manner. However, a transmembrane chemical gradient can bias the Brownian fluctuations in the polypeptide chain toward productive, or rectified, unidirectional translocation. Protonation or deprotonation of acidic side-chains comprising the translocating polypeptide can occur on either the *cis* or the *trans* side of the membrane and decrease or increase, respectively, the energy barriers for entry of the translocating polypeptide into the pore. This model is essentially electrostatic by nature. Given that the PA translocase pore is cation-selective,[9] we expect the LF_N anionic side-chains to play a significant role in the proposed ratchet model.

First, consider that the titrated residues are Asp or Glu (of which there are 54 in LF_N; Figure 9(a)). The LF_N acidic residues are chosen as they are anionic (when deprotonated) and have low p*K* near 4 in solution. The p*K* can be elevated several units in desolvated environments, however, such as the narrow β barrel of the channel or the desolvated interior of the MG form.[3] Since the rate of LF_N translocation increases with increasing $+\Delta\psi$,[4] and LF_N has more negatively charged residues than positively charged residues, we expect that the negative charges are neutralized in stretches of polypeptide as they traverse the channel. In fact, we have shown here that the translocating chain most exposed to the Δψ gradient has a+3 charge dependence in the translocation rate (Figure 6(b)), requiring neutralization of anionic charges in almost any part of the LF_N primary sequence, excepting the most N-terminal end, which is likely not limiting to translocation (Figure 9(a)). Finally, anion-neutralized stretches of translocating polypeptide would be favored in the cation-selective portion of the PA_{63} channel.

In this model, a stretch of anionic polypeptide sequence from LF ($LF^{(-)}_{cis}$) resides initially in the *cis* chamber of the channel and may enter the cation-selective portion of the channel once it is protonated and enough negative charge is neutralized to make the stretch neutral or net-cationic ($LF^{(+)}_{PA63}$). As the $LF^{(+)}_{PA63}$ stretch exits the channel it may then deprotonate, making $LF^{(-)}_{trans}$. The rates at which these stretches of anion-neutralized polypeptide both enter and exit the cation-selective portion of the channel from either the *cis* or the *trans* side are linked to the pH-dependent, microscopic rates of protonation and deprotonation. Under favorable ΔpH conditions ($pH_{trans} > pH_{cis}$), low pH_{cis} drives formation of the intermediate $LF^{(+)}_{PA63}$ species. $LF^{(+)}_{PA63}$ then partitions productively to $LF^{(-)}_{trans}$ and translocates, because protonation is slower in the higher pH of the *trans* solution, and a single cycle of translocation is completed:

$$LF^{\ominus}_{cis} \overset{\text{low } pH_{cis}}{\rightleftharpoons} LF^{\oplus}_{PA63} \overset{pH_{trans} > pH_{cis}}{\rightleftharpoons} LF^{\ominus}_{trans}$$

When the ΔpH conditions are unfavorable ($pH_{trans} < pH_{cis}$), retrograde translocation is more

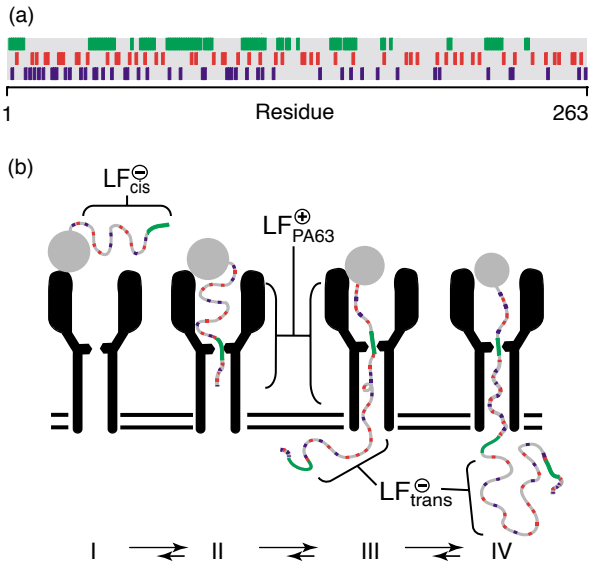

Figure 9. A tandem Brownian ratchet translocation mechanism. (a) Chemical complexity of a protein substrate, LF_N (residues 1–263), colored by functionality: hydrophobic (green), greater than -1.75 kcal mol^{-1} in solvation energy for a ten residue average;[31] cationic (blue), Arg, His or Lys; and anionic (red), Asp or Glu. (b) Depicted is a model of some possible partially unfolded intermediates of LF_N populated during translocation, illustrating how the hydrophobic, ϕ-clamp ratchet and the protonation-state ratchet may work together on a chemically complex protein substrate (as shown in (a)). Stage I: Initially, the amino terminus of LF_N is outside the channel and negatively charged residues are in a deprotonated state, $LF_{cis}^{(-)}$. Stage II: A conductance-blocked intermediate forms when hydrophobic, aromatic and/or cationic sequence binds the ϕ clamp site, which is the narrow constriction on the *cis* side of the extended β barrel[5,10] that effectively maintains the ΔpH. Negatively charged residues in the translocating chain that have entered the channel are protonated, making the stretch net-positive, $LF_{PA63}^{(+)}$; this chain is then compatible with the cation-selective channel. Stage III: The translocating chain proceeds through the ϕ-clamp site as hydrophilic sequence enters the β barrel and exits to the *trans*-side solution (*via* either electro-diffusive or Brownian thermal fluctuations.) Translocation is favored over retro-translocation to the *cis* side under a +ΔpH. Stage IV: Successive iterations of this ΔpH-driven, charge-state ratchet lead to processive translocation.

likely, because the probability that the translocated species, $LF_{trans}^{(-)}$, is populated is decreased, and $LF_{PA63}^{(+)}$ and $LF_{cis}^{(-)}$ accumulate:

$$LF^{\ominus}_{cis} \overset{\text{low } pH_{cis}}{\rightleftharpoons} LF^{\oplus}_{PA63} \overset{pH_{trans} < pH_{cis}}{\rightleftharpoons} LF^{\ominus}_{trans}$$

Thus, under appropriate ΔpH driving force, the charge-state ratchet acts processively upon individual frames of translocating polypeptide sequence rich in acidic residues. In a sense, the channel is functioning as a proton/protein symporter. This translocation model is kinetically linked to the relative kinetic rates of protonating acidic residues and not simply to their thermodynamic pK values. As the kinetic rate of protonating acidic residues is dependent on pH (or specifically $[H^+]$ and $[OH^-]$), this model is consistent with two distinguishing characteristics of the phenomenon: (i) positive ΔpH conditions even at near-neutral *cis* pH are still effective in driving translocation (Figure 5); (ii) negative ΔpH values cause protein translocation to slow abruptly even at low *cis* pH, which destabilize the LF_N tertiary structure (Figure 4). While the LF_N translocation $t_{1/2}$ values (1 to 10 s) are incomparably slower than the protonation timescales ($<10^{-3}$ s) expected for Asp or Glu side-chains in neutral pH buffer, the translocation rate hinges on the timescale of the Brownian diffusion constant of the unfolded protein within the confines of the narrow translocase channel (or possibly on the rate of protein unfolding on the *cis* side). This friction imposed by the channel may severely reduce the overall timescale of translocation.

A previous study[16] has elegantly demonstrated a basic ratchet model for chaperone-assisted translocation through a translocase pore. The rate of translocation (or velocity) is favorably modulated by either the *cis* dissociation rate (k_-) or the *trans* association rate (k_+) of chaperone proteins, which bind sites contained in the translocating chain. These sites would be analogous to proton-binding sites on acidic side-chains in LF_N. Their molecular mechanics model indicated that either increasing k_- or k_+ effectively increased the observed rate of translocation. The model described here is novel, in that the ΔpH-driven charge-state ratchet results not from pH-dependent differences in substrate polypeptide folding, or "coiling," as suggested,[16] but rather from electrostatic repulsion between the channel and anionic charges in the translocating chain, as reflected in the cation-selectivity of the channel.

Tandem synergistic ratchets

Experimental evidence presented in Figure 7 and Table 2 indicates that the ΔpH-driven charge-state ratchet works in conjunction with the ϕ clamp, which we proposed earlier to be a hydrophobic ratchet (Figure 9(b)). The tandem ratchets provide two distinct strategies of interacting with a chemically complex polypeptide substrate that has hydrophobic, hydrophilic, anionic and cationic functionalities distributed across its sequence (Figure 9(a)). For example, during a cycle of translocation, the ϕ clamp located *cis* to the extended β barrel[5,10] can stably bind hydrophobic sequence from the translocating polypeptide. Hydrophilic polypeptide accumulated as a more compact conformer, such as an α helix, in the *trans*-side β barrel may be translocated as an extended conformer *via* the ΔpH-driven, charge-state ratchet, which we expect operates *trans* to the β barrel. In turn, the charge-state ratchet imposes force upon the extended translocating chain and may subsequently induce upstream hydrophobic sequence

to dissociate from the ϕ clamp, thereby completing a cycle of translocation (Figure 9(b)).

Physiological relevance of ΔpH-driven translocation

A translocase in the thylakoid membrane of the chloroplast can transport substrates across membranes *via* a ΔpH-dependent mechanism.[17] The ΔpH-driven translocation in the thylakoid, which is independent of the secretase, Sec61p, as well as NTP hydrolysis, occurs through the twin-arginine translocation system (TAT) and, unlike anthrax toxin, it is not believed to be coupled with the unfolding of substrate proteins.[18] The lack of an unfolding requirement in the TAT system reflects the fact that the translocase forms much larger pores, as shown in electron microscopy studies.[19] The translocase of the mitochondrial inner membrane forms a narrow pore and can translocate sufficiently under either a ΔpH or a Δψ alone (created by a potassium-diffusion potential[20]).

The interchangeability of the Δψ and ΔpH in mitochondria is somewhat analogous to anthrax toxin. The route of anthrax toxin entry into the cell requires endocytosis into vesicles that acidify as they mature.[21] Although the sign of the Δψ in an acidified endosome is certainly positive ($\psi_{endosome} > \psi_{cytosol}$), the reported magnitude varies widely from +10 to +300 mV; the Δψ is highly dependent on the concentration of chloride ions, which have been shown to concentrate in the endosome as it acidifies, lowering the expected Δψ to +10 to +30 mV.[22–24] The ΔpH across the endosomal membrane is more certain, and drugs or mutations in the cellular machinery that block endosomal acidification affect the toxicity of anthrax toxin and other analogous toxins.[21,25]

Experimental evidence presented here demonstrates that a ΔpH promotes anthrax toxin translocation through PA_{63} channels in planar lipid bilayers and suggests that it is likely a principle driving force of translocation in cells. The ΔpH driving force would be expected to be greater in late endosomes (i.e. $pH_{endosome} \approx 5.5$ and $pH_{cytosol} = 7.3$). At pH 5.5, LF_N can be translocated rapidly in planar bilayers at a Δψ of +50 mV and no ΔpH, or alternatively with little or no Δψ (as low as +5 mV) and a ΔpH of one unit. Full-length LF, on the other hand, is unable to be translocated at an appreciable rate, even at +70 mV, in the absence of a ΔpH, and a ΔpH is required to observe significant translocation. Thus, it appears that ΔpH-driven translocation is more relevant to the biological action of the toxin.

In the amino acid sequence of the natural substrates of the PA_{63} translocase, there is a roughly equal proportion of basic, positively charged residues and acidic, negatively charged residues. This argues that, on the one hand, the acidic residues must be protonated for a +Δψ to effectively drive translocation. On the other hand, it is apparent from these ΔpH studies that these acidic residues may play a role in driving translocation, by the proposed ΔpH charge-state ratchet model, and their inclusion in the sequences suggests they are integral to the physiological mechanism of translocation.

Materials and Methods

Proteins

PA (83 kDa) and its mutants, full-length EF, and LF_N (residues 1–263 of LF) and its mutants were expressed recombinantly and purified as described.[3–5,26] The amino-terminal His_6 affinity tags were removed from LF_N and its mutants by treatment with bovine α-thrombin (10 units/mg of protein) for 4 h at room temperature in 20 mM Tris–HCl (pH 8), 150 mM NaCl. Full-length, recombinant LF freed of its His_6 expression tag was provided by Merck Research Laboratories, and was prepared by them as described.[27] LF_N* (LF_N K14C N242C fluorescently labeled with Cys-reactive Alexa Fluor 488 and 546 $C_{(5)}$ maleimides (Molecular Probes)) was prepared as described.[3] LF_N-biotin was prepared by covalently modifying LF_N N242C with a Cys-reactive biotinylation reagent (Pierce), which leaves a disulfide bond between the biotinyl moiety and the protein that is cleavable with a reducing agent such as Tris(2-carboxyethyl)-phosphine (TCEP).[13] The heptameric prepore form of PA_{63} was prepared by nicking PA_{83} with trypsin and purifying the PA_{63} heptamer from the smaller 20 kDa fragment using anion-exchange chromatography.[28]

Planar lipid bilayers

Bilayers were formed by the brush technique[29] across either a 500 μm aperture in a Teflon partition or a 200 μM aperture in a Delrin cup (Warner Instruments, Hamden, CT). Membranes separated two compartments of either 3 ml or 1 ml containing buffered solutions of 100 mM KCl, which could be stirred by small magnetic bars. The buffers used were either 5 mM potassium succinate, 10 mM potassium dimethylglutaric acid (DMG), or universal bilayer buffer (UBB; containing 10 mM oxalic acid, 10 mM Mes, and 10 mM phosphoric acid). All solutions contained in addition 1 mM EDTA. Solution pH values were changed by additions of appropriate amounts of 0.2 M or 2 M KOH, 0.1 M or 1 M HCl, or concentrated buffers of Ches or potassium phosphate. Agar salt-bridges (3 M KCl, 3% agar) linked Ag/AgCl electrodes in 3 M or saturated KCl baths to the *cis* and *trans* compartments. The membrane-forming solution was 3% diphytanoylphosphatidylcholine (Avanti Polar Lipids, Alabaster, AL) in *n*-decane, and membrane formation was monitored either visually or by capacitance. All experiments were done under voltage-clamp conditions; voltages are those of the *cis* solution (to which protein was added) with respect to the *trans* solution, which was held at virtual ground. Current responses were either filtered at 10 Hz and recorded on a Narco physiograph chart recorder (Houston, TX), or filtered at 100 Hz by a low-pass eight-pole Bessel filter (Warner Instruments) and recorded by computer *via* an Instrutech analog-to-digital converter (Instrutech, Port Washington, NY) using AXOGRAPH 4.0 (Axon Instruments, Union City, CA) software.

PA_{63} channel formation and LF, EF or LF_N conductance block

Following membrane formation, PA_{63} prepore heptamer was added to the *cis* compartment, to a final concentration of ~1 ng/ml (~2 pM), which was held at a $\Delta\psi$ of +1 to +20 mV with respect to the *trans* compartment. LF or LF_N was added to the *cis* compartment (final concentration ~3 nM) after PA_{63} channel formation stabilized. The progress of LF, EF or LF_N binding to PA_{63} channels was monitored by the continuous fall of conductance. In most experiments, >95% of the conductance was blocked by LF, EF or LF_N before translocation experiments were begun.

Voltage-step translocation experiments

After LF, EF or LF_N conductance block of PA_{63} channels was complete, excess ligand was removed from the *cis* compartment by perfusion, using a pair of syringes configured in a push/pull arrangement that were driven either manually or automatically by a Hamilton Microlab titrator. The exchange of more than six volumes was accomplished in several minutes, while $\Delta\psi$ was held constant at from +1 to +20 mV. Translocation of LF, EF or LF_N was initiated by stepping $\Delta\psi$ to $\geq +40$ mV.

ΔpH-jump translocation experiments

After LF, EF or LF_N conductance block of PA_{63} channels was complete, excess ligand was removed from the *cis* compartment with perfusion, and translocation was initiated or stimulated by jumping pH_{trans} by adding to the *trans* compartment an appropriate amount of 0.2 M or 2 M KOH, 0.1 M or 1 M HCl, or other concentrated buffer such as Ches or phosphate. Altered pH values were confirmed *in situ* using a micro pH electrode.

Fluorescence equilibrium denaturation

Guanidine hydrochloride denaturation profiles of LF_N* in UBB at pH 7.5 in the presence and absence of 1 M D-glucose were measured using a computer-controlled Hamilton Microlab titrator interfaced to an ISS K-2 fluorimeter for fluorescence resonance energy transfer (Ar^+ laser excitation at 488 nm, emission ratio of 520–570(±16) nm) as described.[3]

Acknowledgements

This work was supported by an NRSA fellowship, AI062204 (to B.A.K), and NIH grants, AI022021 (to R.J.C.) and GM29210 (to A.F.) We thank Roman Melnyk for helpful advice and Charles Peskin for useful discussions of Brownian ratchets. R.J.C. holds equity in PharmAthene, Inc.

Supplementary Data

Supplementary data associated with this article can be found, in the online version, at doi:10.1016/j.jmb.2005.11.030

References

1. Zhao, J. M. & London, E. (1986). Similarity of the conformation of diphtheria toxin at high temperature to that in the membrane-penetrating low-pH state. *Proc. Natl Acad. Sci. USA*, **83**, 2002–2006.
2. Ren, J., Kachel, K., Kim, H., Malenbaum, S. E., Collier, R. J. & London, E. (1999). Interaction of diphtheria toxin T domain with molten globule-like proteins and its implications for translocation. *Science*, **284**, 955–957.
3. Krantz, B. A., Trivedi, A. D., Cunningham, K., Christensen, K. A. & Collier, R. J. (2004). Acid-induced unfolding of the amino-terminal domains of the lethal and edema factors of anthrax toxin. *J. Mol. Biol.* **344**, 739–756.
4. Zhang, S., Udho, E., Wu, Z., Collier, R. J. & Finkelstein, A. (2004). Protein translocation through anthrax toxin channels formed in planar lipid bilayers. *Biophys. J.* **87**, 3842–3849.
5. Krantz, B. A., Melnyk, R. A., Zhang, S., Juris, S. J., Lacy, D. B., Wu, Z. *et al*. (2005). A phenylalanine clamp catalyzes protein translocation through the anthrax toxin pore. *Science*, **309**, 777–781.
6. Koriazova, L. K. & Montal, M. (2003). Translocation of botulinum neurotoxin light chain protease through the heavy chain channel. *Nature Struct. Biol.* **10**, 13–18.
7. Oh, K. J., Senzel, L., Collier, R. J. & Finkelstein, A. (1999). Translocation of the catalytic domain of diphtheria toxin across planar phospholipid bilayers by its own T domain. *Proc. Natl Acad. Sci. USA*, **96**, 8467–8470.
8. Collier, R. J. & Young, J. A. (2003). Anthrax toxin. *Annu. Rev. Cell Dev. Biol.* **19**, 45–70.
9. Blaustein, R. O., Koehler, T. M., Collier, R. J. & Finkelstein, A. (1989). Anthrax toxin: channel-forming activity of protective antigen in planar phospholipid bilayers. *Proc. Natl Acad. Sci. USA*, **86**, 2209–2213.
10. Nassi, S., Collier, R. J. & Finkelstein, A. (2002). PA_{63} channel of anthrax toxin: an extended β-barrel. *Biochemistry*, **41**, 1445–1450.
11. Benson, E. L., Huynh, P. D., Finkelstein, A. & Collier, R. J. (1998). Identification of residues lining the anthrax protective antigen channel. *Biochemistry*, **37**, 3941–3948.
12. Wesche, J., Elliott, J. L., Falnes, P. Ø., Olsnes, S. & Collier, R. J. (1998). Characterization of membrane translocation by anthrax protective antigen. *Biochemistry*, **37**, 15737–15746.
13. Zhang, S., Finkelstein, A. & Collier, R. J. (2004). Evidence that translocation of anthrax toxin's lethal factor is initiated by entry of its N terminus into the protective antigen channel. *Proc. Natl Acad. Sci. USA*, **101**, 16756–16761.
14. Qu, Y., Bolen, C. L. & Bolen, D. W. (1998). Osmolyte-driven contraction of a random coil protein. *Proc. Natl Acad. Sci. USA*, **95**, 9268–9273.
15. Buck, M. (1998). Trifluorethanol and colleagues: cosolvents come of age. Recent studies with peptides and proteins. *Quart. Rev. Biophys.* **31**, 297–355.
16. Simon, S. M., Peskin, C. S. & Oster, G. F. (1992). What drives the translocation of proteins? *Proc. Natl Acad. Sci. USA*, **89**, 3770–3774.
17. Settles, A. M., Yonetani, A., Baron, A., Bush, D. R., Cline, K. & Martienssen, R. (1997). Sec-independent protein translocation by the maize Hcf106 protein. *Science*, **278**, 1467–1470.
18. Hynds, P. J., Robinson, D. & Robinson, C. (1998). The sec-independent twin-arginine translocation system

can transport both tightly folded and malfolded proteins across the thylakoid membrane. *J. Biol. Chem.* **273**, 34868–34874.
19. Gohlke, U., Pullan, L., McDevitt, C. A., Porcelli, I., de Leeuw, E., Palmer, T. *et al*. (2005). The TatA component of the twin-arginine protein transport system forms channel complexes of variable diameter. *Proc. Natl Acad. Sci. USA*, **102**, 10482–10486.
20. Pfanner, N. & Neupert, W. (1985). Transport of proteins into mitochondria: a potassium diffusion potential is able to drive the import of ADP/ATP carrier. *EMBO. J.* **4**, 2819–2825.
21. Friedlander, A. M. (1986). Macrophages are sensitive to anthrax lethal toxin through an acid-dependent process. *J. Biol. Chem.* **261**, 7123–7126.
22. Van Dyke, R. W. & Belcher, J. D. (1994). Acidification of three types of liver endocytic vesicles: similarities and differences. *Am. J. Physiol.* **266**, C81–C94.
23. Rybak, S. L., Lanni, F. & Murphy, R. F. (1997). Theoretical considerations on the role of membrane potential in the regulation of endosomal pH. *Biophys. J.* **73**, 674–687.
24. Sonawane, N. D., Thiagarajah, J. R. & Verkman, A. S. (2002). Chloride concentration in endosomes measured using a ratioable fluorescent Cl^- indicator: evidence for chloride accumulation during acidification. *J. Biol. Chem.* **277**, 5506–5513.
25. Merion, M., Schlesinger, P., Brooks, R. M., Moehring, J. M., Moehring, T. J. & Sly, W. S. (1983). Defective acidification of endosomes in Chinese hamster ovary cell mutants "cross-resistant" to toxins and viruses. *Proc. Natl Acad. Sci. USA*, **80**, 5315–5319.
26. Pimental, R. A., Christensen, K. A., Krantz, B. A. & Collier, R. J. (2004). Anthrax toxin complexes: heptameric protective antigen can bind lethal factor and edema factor simultaneously. *Biochem. Biophys. Res. Commun.* **322**, 258–262.
27. Shoop, W. L., Xiong, Y., Wiltsie, J., Woods, A., Guo, J., Pivnichny, J. V. *et al*. (2005). Anthrax lethal factor inhibition. *Proc. Natl Acad. Sci. USA*, **102**, 7958–7963.
28. Cunningham, K., Lacy, D. B., Mogridge, J. & Collier, R. J. (2002). Mapping the lethal factor and edema factor binding sites on oligomeric anthrax protective antigen. *Proc. Natl Acad. Sci. USA*, **99**, 7049–7053.
29. Mueller, P., Rudin, D. O., Tien, H. T. & Westcott, W. C. (1963). Methods for the formation of single bimolecular lipid membranes in aqueous solution. *J. Phys. Chem.* **67**, 534–535.
30. Blaustein, R. O. & Finkelstein, A. (1990). Voltage-dependent block of anthrax toxin channels in planar phospholipid bilayer membranes by symmetric tetraalkylammonium ions. Effects on macroscopic conductance. *J. Gen. Physiol.* **96**, 905–919.
31. Wesson, L. & Eisenberg, D. (1992). Atomic solvation parameters applied to molecular dynamics of proteins in solution. *Protein Sci.* **1**, 227–235.

Edited by G. von Heijne

(Received 10 October 2005; received in revised form 4 November 2005; accepted 8 November 2005)
Available online 1 December 2005